Translational Oncology

www.transonc.com

Volume 5 Number 2 April 2012 pp. 113–123 113

Down-regulation of *ANAPC13* and *CLTCL1*: Early Events in the Progression of Preinvasive Ductal Carcinoma of the Breast[1,2]

Carolina Sens-Abuázar*, Elisa Napolitano e Ferreira*, Cynthia Aparecida Bueno Toledo Osório†, Ana Cristina Victorino Krepischi‡,§, Tatiana Iervolino Ricca*, Nadia Pereira Castro*, Isabela Werneck da Cunha†, Maria do Socorro Maciel¶, Carla Rosenberg§,#, Maria Mitzi Brentani, Fernando Augusto Soares†, Rafael Malagoli Rocha† and Dirce Maria Carraro*,§**

*Laboratory of Genomics and Molecular Biology, International Center of Research and Teaching, A.C. Camargo Hospital, São Paulo, SP, Brazil; †Department of Investigative Pathology, International Center of Research and Teaching, A.C. Camargo Hospital, São Paulo, SP, Brazil; ‡Laboratory of Cancer Genetics, International Center of Research and Teaching, A.C. Camargo Hospital, São Paulo, SP, Brazil; §National Institute of Science and Technology in Oncogenomics, São Paulo, SP, Brazil; ¶Department of Mastology, A.C. Camargo Hospital, São Paulo, SP, Brazil; #Department of Genetics and Evolutionary Biology, Institute of Biosciences, University of São Paulo, São Paulo, SP, Brazil; **Department of Radiology, Discipline of Oncology, Medical School, University of São Paulo, São Paulo, SP, Brazil

Abstract

Alterations in the gene expression profile in epithelial cells during breast ductal carcinoma (DC) progression have been shown to occur mainly between pure ductal carcinoma *in situ* (DCIS) to the *in situ* component of a lesion with coexisting invasive ductal carcinoma (DCIS-IDC) implying that the molecular program for invasion is already established in the preinvasive lesion. For assessing early molecular alterations in epithelial cells that trigger tumorigenesis and testing them as prognostic markers for breast ductal carcinoma progression, we analyzed, by reverse transcription–quantitative polymerase chain reaction, eight genes previously identified as differentially expressed between epithelial tumor cells populations captured from preinvasive lesions with distinct malignant potential, pure DCIS and the *in situ* component of DCIS-IDC. *ANAPC13* and *CLTCL1* down-regulation revealed to be early events of DC progression that anticipated the invasiveness manifestation. Further down-regulation of *ANAPC13* also occurred after invasion appearance and the presence of the protein in invasive tumor samples was associated with higher rates of overall and disease-free survival in breast cancer patients. Furthermore, tumors with low levels of *ANAPC13* displayed increased copy number alterations, with significant gains at 1q (1q23.1-1q32.1), 8q, and 17q (17q24.2), regions that display common imbalances in breast tumors, suggesting that down-regulation of *ANAPC13* contributes to genomic instability in this disease.

Translational Oncology (2012) 5, 113–123

Address all correspondence to: Dirce Maria Carraro, PhD, CIPE-International Center of Research and Teaching, Laboratory of Genomics and Molecular Biology, A.C. Camargo Hospital, Rua Tagua, 440, CEP 01508-010 São Paulo, SP, Brazil. E-mail: dirce.carraro@cipe.accamargo.org.br

[1]This work was supported by Fundação de Amparo à Pesquisa do Estado de São Paulo (CEPID/FAPESP 98/14335). C.S.A. was supported by CNPq (142790/2008-7) and FAPESP (2009/00669-2). T.I.R. was supported by FAPESP (2009/02457-2). The authors declare no conflicts of interest.

[2]This article refers to supplementary materials, which are designated by Tables W1 to W9 and Figure W1 and are available online at www.transonc.com.

Received 15 September 2011; Revised 16 December 2011; Accepted 21 December 2011

1944-7124/12 DOI 10.1593/tlo.11280

Introduction

Breast carcinoma is a complex disease that displays molecular heterogeneity at both the preinvasive [1–4] and invasive [5,6] stages. Gene expression pattern is mainly influenced by the expression of hormonal receptors, estrogen (ER) and progesterone (PR) and *ERBB2* oncogene, and tumor classification based on expression profile leads to significant repercussion on prognosis [5,6].

Ductal carcinoma (DC) of the breast represents 80% of all breast tumors [7] and can be manifested as *in situ* (DCIS) or as invasive carcinoma (IDC), the latter of which can be present with or without an *in situ* component (DCIS-IDC). DCIS is characterized by the confinement of cells within ducts, maintenance of the basal membrane and lack of stromal invasion. IDC is characterized by the spreading of cancer cells through ducts by crossing the basal membrane, leading to stromal invasion.

DCIS is thought to be a precursor of IDC [8,9], and its progression is not predictable using the currently available resources. Conventional histologic features and biomarkers are not effective for classifying pure DCIS lesions regarding their ability to invade surrounding tissues and, consequently, trigger disease progression.

Cell-based studies have reported negligible differences in gene expression patterns between epithelial cells from IDC and those from the *in situ* component of DCIS-IDC lesions [10–12], suggesting that genetic and molecular abnormalities, important for the acquisition of invasiveness, are already present in preinvasive epithelial cells [10,13–15]. In addition, surrounding myoepithelial cells [16–18] and fibroblast cells [17,19] certainly play a fundamental role in invasion process.

We have previously shown that most of the divergences in gene expression patterns during the course of breast tumor progression occur between epithelial cells from pure DCIS and those from the *in situ* component of DCIS-IDC lesions [10]. Therefore, the assessment of the molecular divergence of epithelial tumor cells of same morphology but with completely different malignant potentials may uncover key molecular events involved in early steps of DC progression.

In this sense, the goal of this study was to investigate the earliest molecular alterations important for acquiring invasive capability and to discover prognostic factors for DC of the breast. Thus, we assessed, by reverse transcription–quantitative polymerase chain reaction (RT-qPCR), the expression of eight candidate genes chosen from our previously published gene expression signature [10], in laser-capture microdissected epithelial tumor cells from pure DCIS and from the *in situ* component of DCIS-IDC lesions. The criterion of gene selection was based on the availability of commercial antibodies for a posterior immunohistochemistry (IHC) analysis. Protein expression was evaluated in a panel of pure DCIS, *in situ* component of DCIS-IDC and IDC lesions. *ANAPC13* and *CLTCL1* were showed to be implicated in the earliest steps of malignant process of tumor cells. *ANAPC13* (anaphase-promoting complex subunit 13) encodes a 74-amino acid protein [20] that participates in the anaphase-promoting complex (APC/C), a large ubiquitin ligase that controls cell cycle progression [21], and it is essential at the metaphase-to-anaphase transition. *CLTCL1* (clathrin, heavy chain-like 1) belongs to the clathrin family and encodes a protein of 1640 amino acids that is highly expressed in muscle tissues [22,23]. Clathrins are essential for intracellular traffic [24,25] and participate in the stabilization of mitotic spindle fibers [26]. The results demonstrated that decreases in *ANAPC13* and *CLTCL1* expression occur before DCIS cells manifest morphologic aspects of invasion. Furthermore, decrease in *ANAPC13* expression seems to be also involved in late stages of tumor progression and in increasing genomic instability. Moreover, the presence of ANAPC13 protein was associated with higher rates of overall survival and disease-free survival in general IDC. Together, these results suggest *ANAPC13* as a promising novel molecular prognostic markers for DC.

Materials and Methods

Samples

Frozen samples from five pure DCIS, 15 *in situ* component of DCIS-IDC and 10 IDC lesions were used for laser microdissection and RT-qPCR (Table 1). An independent set of 42 frozen specimens from IDC lesions was also used. These samples were manually dissected for enrichment of at least 70% of tumor cells. DNA from the same 42 samples was used for mutation screening and from 33 of these 42 was used for array comparative genomic hybridization (aCGH). Total RNA from the 33 samples was used for RT-qPCR. For IHC, an independent set of formalin-fixed paraffin-embedded (FFPE) tumor breast tissues were organized in two tissue microarrays as described [27] (Table W1). TMA1 was composed of 41 pure DCIS and 36 *in situ* component of DCIS-IDC samples, and TMA2 consisted of 187 IDC samples.

For pure DCIS lesions, all slides from each patient were examined by pathologists to ensure the absence of any previously undetected microinvasion. The classification of DCIS samples is in accordance with the World Health Organization guidelines, and the Nottingham (Elston-Ellis) modification of the Scarff-Bloom-Richardson grade system (SBR grade) was applied for IDC samples.

All breast cancer samples were previously analyzed by IHC for the expression of ER (rabbit monoclonal anti-ER, clone SP1; Dako, Carpinteria, CA), PR (mouse monoclonal anti-PR, clone PgR636; Dako), and human epidermal growth factor receptor type 2 (HER2) (rabbit polyclonal anti-HER2, 1:1000; Dako). ER, PR, and HER2 were evaluated according to the recommendations of the American Society of Clinical Oncology and the College of American Pathologists guidelines [28,29]. *HER2* amplification was assessed in positive 2+ IDC samples by fluorescence *in situ* hybridization (FISH) analysis, following the manufacturer's standard methods (Dako), and hybridization was performed with HER2/CEN-17 probes (Dako). Results were interpreted using the algorithm established by the American Society of Clinical Oncology and College of American Pathologists guidelines [29]. IDC samples were classified as luminal A (ER^+ and/or PR^+, $HER2^-$), luminal B (ER^+ and/or PR^+, $HER2^+$), $HER2^+$ (ER^-, PR^-, $HER2^+$), basal-like [ER^-, PR^-, $HER2^-$, cytokeratin (CK) $5/6^+$ and/or epidermal growth factor receptor ($EGFR^+$)], or unclassified (negative for all five markers) according to Perou et al. [5] and Khramtosv et al. [30]. The inclusion criteria were female patients with ductal carcinoma without preoperative systemic treatment. Samples were obtained from the tumor bank and the archives of the Department of Investigative Pathology, A.C. Camargo Hospital Tumor Bank, São Paulo, Brazil. This study was approved by the Ethics Committee of the Medical and Research Center of A. C. Camargo Hospital (1143/08).

RNA/DNA Extraction and RNA Amplification

Approximately 4000 cells were laser captured from frozen tissues of specific component of each breast ductal lesion with PixCell II LCM system (Arcturus Engineering, Mountain View, CA). RNA isolation and amplification were performed as described by Castro et al. [10]. RNA isolation of manually dissected frozen tissues was performed using RNeasy Mini Kit (Qiagen, Germantown, MD). DNA was isolated by incubating in 600 μl of digestion buffer (25 mM EDTA,

Table 1. Characteristics of Patients and Tumors Selected for RT-qPCR Analysis.

Sample Type	Sample Name	Clinical Stage	Age at Diagnosis (Years)	pTNM	Nuclear Grade	SBR Grade	ER Status	PR Status	P53 Status	HER2 Immunostaining
Pure DCIS	1	0	37	Tis N0 M0	ND	–	–	–	+	ND
	2	0	44	Tis N0 M0	2 and 3	–	+	+	–	0
	3	0	43	Tis N0 M0	3	–	+	+	–	(3+)
	4	0	52	Tis N0 M0	3	–	+	+	–	(3+)
	5	0	58	Tis N0 M0	3	–	–	–	–	(3+)
DCIS-IDC*	6	IIa	48	T2 N0 M0	3	II	+	+	+	(1+)
	7	IIa	75	T2 N0 M0	2	II	+	+	+	(2+)
	8	IIa	34	T1c N0 M0	3	II	+	+	+	(3+)
	9	I	55	T1 N0 M0	3	ND	–	–	+	(3+)
	10	IIIb	44	T4b N1 M0	2	III	+	+	ND	(2+)
	11	IIb/IIa	57	T2 N2 M0	2	II	+	+	ND	(2+)
	12	IIb	43	T2 N0 M0	2	II	–	–	+	(3+)
	13	IIa	48	T2 N0 M0	2	II	+	+	–	(2+)
	14	I	73	T3 N0 M0	2	II	+	+	–	(2+)
	15	ND	46	T2 N1 M0	3	II	+	+	+	(2+)
	16	IIa	48	T2 N1 M0	3	II	–	–	–	(2+)
	17	ND	63	T2 N0 M0	1	ND	+	–	–	(2+)
	18	ND	39	T1c N0 M0	ND	ND	+	+	ND	(3+)
	19	ND	49	T1c N0 M0	ND	ND	+	+	ND	(0)
	20	IIb	69	T2 N1 M0	ND	ND	+	+	ND	(2+)
IDC	21	IIa	45	T2 N0 M0	2	II	–	–	–	(3+)
	22	IIa	43	T1c N0 M0	3	II	+	–	–	(3+)
	23	IIa	54	T2 N0 M0	3	II	+	+	+	(3+)
	24	IIIb	71	T4 N2 M0	3	III	+	+	+	(2+)
	25	IIa	43	T2 N0 M0	3	III	–	ND	ND	(3+)
	26	IIIa	43	T2 N2 M0	3	III	+	+	ND	(2+)
	27	I	ND	ND	ND	ND	ND	ND	ND	ND
	28	IIa	44	T1 N1 M0	3	II	+	+	–	(1+)
	29	IIb	31	T2 N1 M0	3	II	–	–	+	(3+)
	30	IIIa	54	T3 N1 M0	3	III	–	–	–	(2+) (1+)

DCIS indicates ductal carcinoma *in situ*; DCIS-IDC, ductal carcinoma *in situ* with coexisting invasive ductal carcinoma; ER, estrogen receptor; HER2, human epidermal growth factor receptor type 2; ND, not determined; PR, progesterone receptor; pTNM, pathologic tumor size, nodal status, and metastasis.
*DCIS-IDC samples were classified according to the IDC lesion.

pH 8.0, 0.25% of sodium dodecyl sulfate, 100 mM NaCl, 100 mM Tris-HCl, pH 8.0 and 300 μg of proteinase K) at 55°C overnight, followed by 100% ethanol precipitation, and 70% ethanol washes, and DNA was recovered in Tris-EDTA, pH 8.0.

RT-qPCR

Complementary DNA converted from 1 μg of amplified RNA (aRNA) or total RNA, purified from laser-capture microdissected cells or manually dissected IDC tissues, respectively, was used as template for RT-qPCR analysis. RT-qPCRs were performed using the ABI Prism 7900HT Fast Real-time Sequence Detection System (Applied Biosystems, Foster City, CA). Reactions were carried out in duplicates using SYBR Green PCR MasterMix (Applied Biosystems) in a total volume of 20 μl. Dissociation curves were analyzed for each primer pair to verify the specificity of the RT-qPCR reaction. Only samples with differences $\leq$0.6 in quantification cycle (Cq) between duplicates were considered for the analysis. Five endogenous control genes, *ACTB*, *BCR*, *GAPDH*, *HPRT1*, and *RPLP0* were evaluated. The two most stable endogenous genes (*HPRT1* and *RPLP0*) were selected by using geNorm [31]. Relative gene expression quantification was calculated using the efficiency-corrected equation [32]. The list of primers used is shown in Table W2.

Immunohistochemistry

IHC was performed as previously described [27]. Slides were incubated with the following primary antibodies: mouse monoclonal anti-ADFP (clone aa5-27, 1:50, Life Span Biosciences, Seattle, WA), rabbit polyclonal anti-ANAPC13 (1:30; Sigma Aldrich, St. Louis, MO), goat polyclonal ARHGAP19 (1:50; Santa Cruz Biotechnology, Santa Cruz, CA), and mouse monoclonal anti-CLTCL1 (clone 2Q2166, 1:300; Abcam, Cambridge, MA) for 2 hours. Samples stained without the primary antibody were used as negative controls. Normal breast tissues, known to express these proteins, according to the Human Protein Atlas were used as positive controls. Samples were analyzed microscopically (Axioskop 40; Carl Zeiss Co, Tokyo, Japan) by a pathologist. Nuclear and cytoplasmic staining patterns were considered in the analysis when detected in at least 10% of the cells. Nuclear staining was classified using the Allred score (scores 0-8) [33]. Samples were categorized as negative (scores 0-3) or positive (scores 4-8). Cytoplasmic staining was considered as absent, weak, moderate, and strong staining. For determining the correspondence between messenger RNA (mRNA) and protein, samples were categorized as negative (absent and weak) or positive (moderate and strong).

ANAPC13 and CLTCL1 Antibody Specificity

For both proteins, ANAPC13 and CLTCL1, Western blot assays were performed for assessing antibodies specificity as described [34]. Proteins were detected using rabbit polyclonal anti-ANAPC13 (1:500; Sigma Aldrich) and mouse monoclonal anti-CLTCL1 (clone 2Q2166, 1:150; Abcam) antibodies. Signals were detected using ECL horseradish peroxidase–conjugated immunoglobulin G whole antibodies (1:1500; GE Healthcare, Little Chalfont, United Kingdom). Proteins from MCF7 (HTB-22) and SK-BR-3 (HTB-30) human breast cancer cell lines (American Type Culture Collection, ATCC, Manassas, VA) were used. Cell lines were propagated following ATCC recommendations.

ANAPC13 *Mutation Screening*

Primers corresponding to all exonic regions and also the exon/intron borders of *ANAPC13* were designed (Table W2). *ANAPC13* mutation screening was performed for the 42 frozen IDC samples. PCR products were confirmed by agarose gel electrophoresis and sequenced using the 3130XL Genetic Analyzer (Applied Biosystems, Foster City, CA). For all samples, sequences were obtained using both forward and reverse primers and analyzed in CLC DNA Genomics Workbench software 4.5 (CLCbio, Katrinebjerg, Denmark), using RefSeq NM_015391.3 as reference.

Investigation of Copy Number Alterations by Whole Genome Comparative Genomic Hybridization on Microarrays

Array CGH (aCGH) investigation was performed on 33 of the 42 frozen IDC samples by oligonucleotide array CGH using whole-genome platforms from Agilent Technologies (Agilent SurePrint G3 Human CGH Microarrays 8×60K [containing 60,000 oligonucleotides probes] and 4×180K [containing 180,000 oligonucleotides probes]). Briefly, samples were labeled with Cy3- and Cy5-dCTPs by random priming, and purification, hybridization, and washing were carried out as recommended by the manufacturer. Scanned images of the arrays were processed using Feature Extraction software (Agilent Technologies, Santa Clara, CA), and the analysis was carried out using Nexus Copy Number 5.1 (Biodiscovery, El Segundo, CA). For aCGH analysis, identification of aberrant copy number segments was based on FASST2 segmentation algorithm with default settings (threshold $\log_2$ ratio of 0.2 or 1.14 was used for gain or high copy gain, and −0.23 and −1.14 used for loss and homozygous loss, respectively), and the significance threshold was set on 1.0^{-7}. We considered at least three consecutive probes for calling a segment, and a filter against aberrations smaller than 150 kb was used.

Statistical Analysis

For RT-qPCR analyses, a criterion of fold change $\geq |2|$ was applied for considering differentially expressed genes. The IHC statistical analyses were performed with STATA software (Intercooled Stata release 7.0; Stata Corporation, College Station, TX). For the categorical variables, the χ^2 or Fisher exact test was applied. Overall survival and disease-free survival probabilities were calculated using the Kaplan-Meier method, and the log-rank test was used to compare survival curves. The Cox regression model was used to estimate relative risks with a confidence interval of 95% and to obtain independent prognostic variables. Results were considered statistically significant when $P < .05$.

Results

Assessment of Gene Expression in Tumor Epithelial Cells from Pure DCIS and the In Situ *Component of DCIS-IDC*

To identify novel molecular markers for the progression of DC of the breast, we explored differences in gene expression that occur in epithelial cells from preinvasive lesions, pure DCIS, and the *in situ* component of DCIS-IDC. Epithelial tumor cells were captured by laser from five pure DCIS and from 15 *in situ* component of DCIS-IDC samples (Figure 1*A* and Table 1). Eight genes (*ADFP*, *ANAPC13*, *ARHGAP19*, *CLTCL1*, *CPNE3*, *IMMT*, *NGDN*, and *PIAS2*) selected from our previous study [10], were assessed by RT-qPCR in both cell populations, pure DCIS, and the *in situ* component of DCIS-IDC. For this analysis, complementary DNA was converted from amplified RNA and used for RT-qPCR experiments because no introduction of bias in relative gene expression was previously detected [35]. Four genes showed concordant results between RT-qPCR and microarray data [10], *ADFP* (RT-qPCR fold change = 2.79), *ANAPC13* (RT-qPCR fold change = 2.00), *ARHGAP19* (RT-qPCR fold change = 6.88), and *CLTCL1*

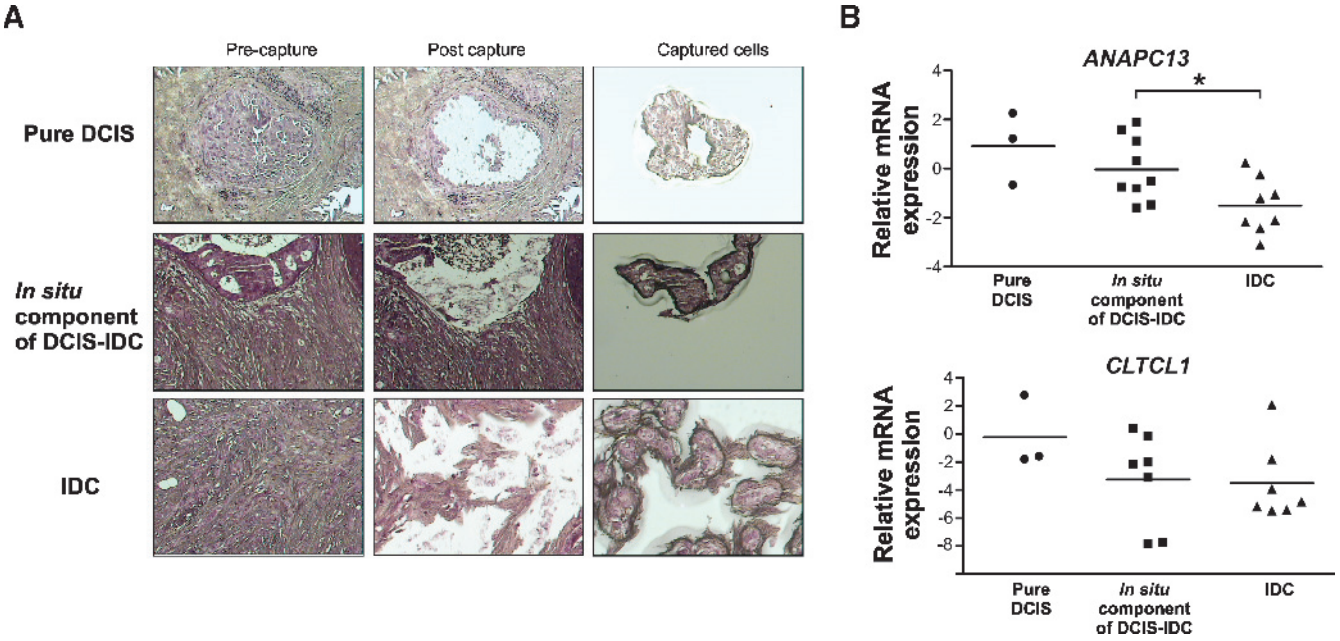

Figure 1. mRNA down-regulation of *ANAPC13* and *CLTCL1* along the progression of epithelial tumor cells of the breast. (A) Breast epithelial cells captured from pure DCIS, *in situ* component of DCIS-IDC and IDC lesions by laser-capture microdissection. Original magnifications, ×100. (B) Relative mRNA expression of *ANAPC13* and *CLTCL1* in pure DCIS, *in situ* component of DCIS-IDC and IDC. DCIS indicates ductal carcinoma *in situ*; DCIS-IDC, ductal carcinoma *in situ* with coexisting invasive ductal carcinoma; IDC, invasive ductal carcinoma. *$P < .05$.

Table 2. ANAPC13 and CLTCL1 Expression (Cytoplasmic Staining) in a Tissue Microarray Composed of *In Situ* Lesions.

Variable	Category	ANAPC13, *n* (%)*		*P*	CLTCL1, *n* (%)*		*P*
		Negative	Positive		Negative	Positive	
Histologic type of DCIS	Pure DCIS	11 (30.50)	25 (69.50)	.02†	14 (40.00)	21 (60.00)	.04†
	In situ component of DCIS-IDC	16 (59.20)	11 (40.80)		20 (64.50)	11 (35.50)	
Histologic subtype	Non-comedo	21 (41.20)	30 (58.80)	.42	29 (54.70)	24 (45.30)	.09
	Comedo	6 (54.60)	5 (45.40)		3 (27.30)	8 (72.70)	
Nuclear grade	Non-high grade	14 (41.20)	20 (58.80)	.49	19 (57.60)	14 (42.40)	.26
	High grade	13 (50.00)	13 (50.00)		13 (43.30)	17 (56.70)	
Histologic grade	Non-high grade	12 (38.70)	19 (61.30)	.32	18 (60.00)	12 (40.00)	.19
	High grade	13 (52.00)	12 (48.00)		12 (42.90)	16 (57.10)	
ER status	Negative	12 (75.00)	4 (25.00)	<.01‡	11 (57.90)	8 (42.10)	.46
	Positive	12 (30.80)	27 (69.20)		19 (47.50)	21 (52.50)	
PR status	Negative	18 (62.10)	11 (37.90)	<.01‡	16 (50.00)	16 (50.00)	.88
	Positive	6 (23.10)	20 (76.90)		13 (48.20)	14 (51.80)	
HER2 status	Negative	4 (57.00)	3 (43.00)	.68	5 (63.00)	3 (38.00)	.46
	Positive	21 (44.00)	27 (56.00)		22 (47.00)	25 (53.00)	

DCIS indicates ductal carcinoma *in situ*; DCIS-IDC, ductal carcinoma *in situ* with coexisting invasive ductal carcinoma; ER, estrogen receptor; HER2, human epidermal growth factor receptor type 2; PR, progesterone receptor.
*Percentage considering number of cases with complete information.
†*P* value < 0.05.
‡*P* value < 0.01.

(RT-qPCR fold change = 6.25) displaying up-regulation in pure DCIS cells. The remaining four genes did not fullfill the adopted criterion differences in expression levels between epithelial cells from pure DCIS and those from the *in situ* component of DCIS-IDC.

Assessment of Protein Expression in Pure DCIS and in the In Situ *Component of DCIS-IDC*

To assess protein expression, samples from 41 pure DCIS lesions and 36 *in situ* component of DCIS-IDC lesions (TMA1) were stained with antibodies against ADFP, ANAPC13, ARHGAP19, and CLTCL1 and evaluated by IHC. ADPF and CLTCL1 showed cytoplasmic staining, whereas ANAPC13 and ARHGAP19 showed both nuclear and cytoplasmic staining. Samples were categorized as negative (absent or weak staining) or positive (moderate or strong staining). Results of cytoplasmic staining for ANAPC13 and CLTCL1 were concordant with those observed at the mRNA level (Figure 1*B*). Positive ANAPC13 was detected in 69.5% of pure DCIS samples and in 40.8% of *in situ* component of DCIS-IDC samples ($P = .02$). Positive CLTCL1 was detected in 60.0% of pure DCIS samples and in 35.5% of *in situ* component of DCIS-IDC samples ($P = .04$; Table 2). In contrast, no statistically significant differences were found in cytoplasmic staining for ADFP and ARHGAP19 and nuclear staining for ANAPC13 and ARHGAP19 between pure DCIS and *in situ* component of DCIS-IDC samples (Table W3). Assessment of associations between immunostaining patterns and clinicopathologic variables (Table 2) demonstrated statistically significant associations between positive cytoplasmic ANAPC13 samples and positive status for ER and PR ($P < .01$).

To better characterize the protein sublocation of ANAPC13 and CLTCL1, we firstly assessed the antibodies specificity (Figure 2) and then evaluated 10 entire lesions (5 pure DCIS and 5 *in situ* component of DCIS-IDC lesions) using ScanScope XT scanner (Aperio, Vista, CA). Sharp patterns of nuclear and/or cytoplasmic staining were observed for ANAPC13. For CLTCL1, staining was mainly cytoplasmic with some membrane staining. No nonspecific stromal or parenchymal staining was observed for either antibody (Figure 2).

Assessment of the Transcriptional Levels of ANAPC13 *and* CLTCL1 *during Tumor Progression*

To assess modulation of *ANAPC13* and *CLTCL1* mRNA levels during the progression of tumor epithelial cells in DC, we evaluated epithelial cells captured from 10 invasive ductal carcinoma samples (IDC) by RT-qPCR. *ANAPC13* mRNA levels progressively decreased in epithelial cells from IDC when compared with cells from the *in situ* component of DCIS-IDC lesions (fold change = 2.78; $P = .02$) (Figure 1*B*). No difference was observed in *CLTCL1* expression between cells from the *in situ* component of DCIS-IDC and IDC cells (fold change = 1.00; $P = .88$) (Figure 1*B*).

Protein Expression of ANAPC13 and CLTCL1 during Tumor Progression

To investigate the protein levels of ANAPC13 and CLTCL1 during DC progression, cytoplasmic expression of both proteins was evaluated in a second TMA (TMA2) composed of 187 IDC tissues. Absent staining was observed in 39.0% of the IDC samples, whereas weak or moderate staining was detected in 40.1% and 20.9% of the cases, respectively. Strong cytoplasmic staining for ANAPC13 was not observed in IDC samples. Absent staining for CLTCL1 was observed in 25.2% of the samples, whereas weak, moderate, and strong staining were detected in 43.6%, 26.2%, and 5.0% of the IDC cases, respectively.

To confirm whether the mRNA and protein expression levels were in agreement during breast cancer progression, we assessed the frequency of samples categorized in IHC as negative (absent and weak staining) and as positive (moderate and strong staining) (Figure 3*A*) in each sample group (pure DCIS, *in situ* component of DCIS-IDC and IDC). Both proteins showed tendencies, similar to those observed at the mRNA level. The frequency of samples classified as positive for ANAPC13 protein was clearly reduced in IDC lesions. The opposite was observed for the samples classified as negative for ANAPC13 (Figure 3*B*). The frequency of positive samples for CLTCL1 was reduced in the *in situ* component of DCIS-IDC when compared with pure DCIS lesions; however, similar frequencies of CLTCL1-positive samples were observed between lesions representative of the *in situ* component of DCIS-IDC and of IDC (Figure 3*B*). Together, these

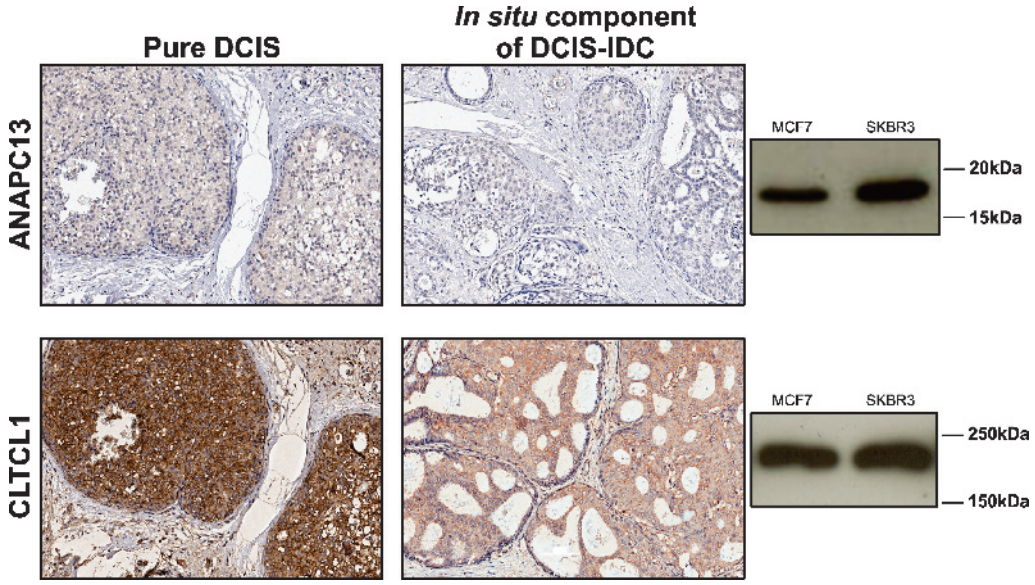

Figure 2. Protein expression of ANAPC13 and CLTCL1 in pure DCIS and in the *in situ* component of DCIS-IDC. Immunohistochemical staining, showing higher expression of ANAPC13 and CLTCL1 proteins in lesions representative of pure DCIS (left) and *in situ* component of DCIS-IDC (right). Level of background or nonspecific staining, sharpness, intensity, and localization were considered in the IHC analysis. Antibody specificity determined by Western blot for ANAPC13 (19 kDa) and for CLTCL1 (192 kDa) (right panel). Images acquired from ScanScope XT scanner (Aperio). Original magnifications, ×200. DCIS indicates ductal carcinoma *in situ*; DCIS-IDC, ductal carcinoma *in situ* with coexisting invasive ductal carcinoma; MCF7 and SKBR-3, human breast cancer cell lines.

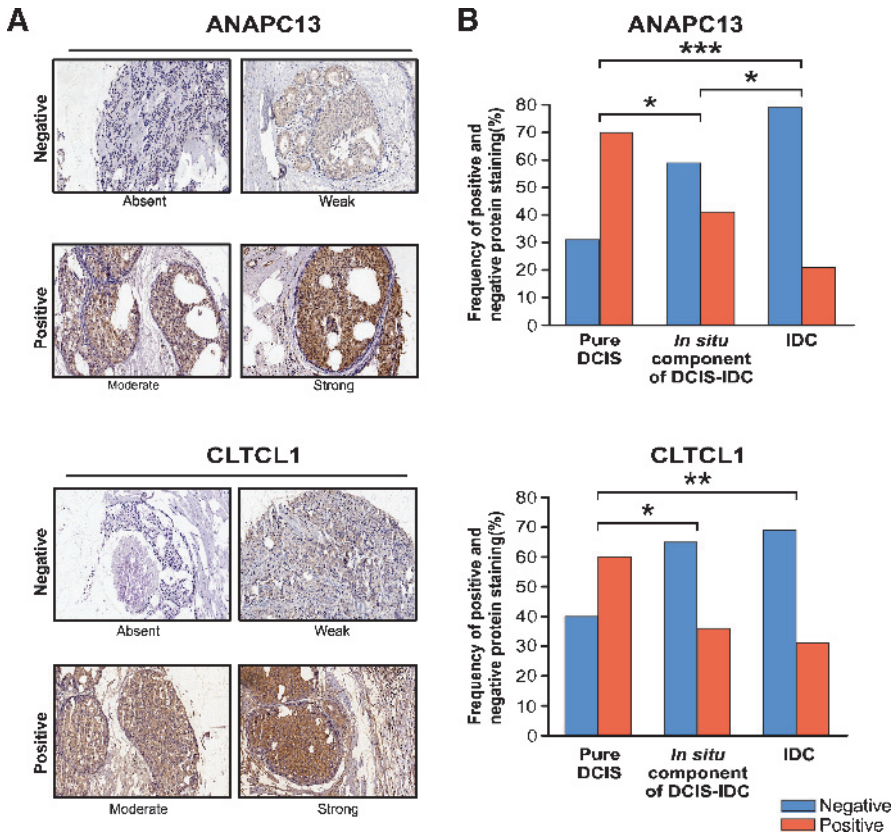

Figure 3. Frequency of positive and negative protein staining of ANAPC13 and CLTCL1 along DC progression. (A) Immunohistochemical analysis of ANAPC13 and CLTCL1, showing examples of the immunostaining pattern categorized as negative (absent and weak staining) and positive (moderate and strong staining). For ANAPC13, strong staining was only observed in DCIS lesions. Images acquired from ScanScope XT scanner (Aperio). (B) Graph bars representing the frequency of positive and negative protein staining of ANAPC13 and CLTCL1 in pure DCIS, *in situ* component of DCIS-IDC, and IDC lesions, respectively. DC indicates ductal carcinoma; DCIS, ductal carcinoma *in situ*; DCIS-IDC, ductal carcinoma *in situ* with coexisting invasive ductal carcinoma; IDC, invasive ductal carcinoma. *$P < .05$, **$P < .01$, ***$P < .001$.

results suggest that the down-regulation of *ANAPC13* may be involved not only in early molecular alterations that precede the morphologic manifestation of invasion but also in late stages in the progression of epithelial cells of DC, whereas, down-regulation of *CLTCL1* seems to be an early event that anticipates the invasive phenotype and that occurs at a defined time during DC progression.

ANAPC13 and CLTCL1 as Prognostic Factors for Invasive Ductal Carcinoma

We next tested the prognostic potential of ANAPC13 and CLTCL1 by analyzing possible associations of these proteins with the clinicopathologic variables of the IDC samples. No statistically significant associations were observed between protein staining patterns and clinicopathologic variables (Table 3). Next, univariate analysis was performed to assess the association of cytoplasmic staining of ANAPC13 and CLTCL1 with overall and disease-free survival in patients with invasive breast carcinoma (Table W4) categorizing as negative, absent staining, and positive, weak, moderate, and strong staining. Overall and disease-free survival rates were higher among patients with positive cytoplasmic expression of ANAPC13 (log-rank test, $P = .003$ and $P = .04$, respectively; Figure 4, *A* and *B*). These results strongly suggest the potential of ANAPC13 as a favorable prognostic factor in IDC. According to the Cox regression univariate model, patients with negative ANAPC13 cytoplasmic tumors had a two-fold higher risk of dying than patients with tumors positive for this protein (crude hazard ratio = 2.00, 95% confidence interval = 1.3-3.2). Multivariate analysis demonstrated that ANAPC13 is an independent prognostic factor (hazard ratio = 2.09, 95% confidence interval = 1.3-3.4), reinforcing it as a promising molecular marker for IDC (Table W5).

Finally, we classified the IDC samples based on their molecular subtypes as luminal A ($n = 106$), luminal B ($n = 12$), HER2$^+$ ($n = 19$), basal-like ($n = 12$), and unclassified ($n = 19$) lesions (Tables W6 and W7) as defined in Materials and Methods. Only luminal A subtype showed a significant association between positive ANAPC13 and the presence of three or less compromised lymph nodes ($P = .0158$). In addition, among luminal A samples, the overall survival rate was higher for patients with positive ANAPC13 samples (log-rank test, $P = .004$; Figure 4*C*). No significant associations were found between ANAPC13 staining categories and disease-free survival in luminal A cases (Figure 4*D*) as well as for overall and disease-free survival rates in the other molecular subtypes.

Mutation Screening in ANAPC13 *Gene*

Given that *ANAPC13* down-regulation seems to play an important role during DC progression, we evaluated whether protein interruption causing mutations in *ANAPC13* could lead to decreased expression during late stages of tumor progression. Thus, the three exons, two of them coding, and the exon/intron borders of *ANAPC13* were analyzed by DNA sequencing in 42 IDC samples. Seven alterations were found, but none of them were within the coding sequence indicating that mutation may not be the event that contributes to the decrease or absence of ANAPC13 protein in breast tumor (Table W8 and Figure W1*A*).

Copy Relation of ANAPC13 *Expression and Copy Number Alterations*

We reasoned that decrease of *ANAPC13* could result in genomic instability during breast tumor progression. To test this hypothesis, we classified a group of 33 IDC samples based on their *ANAPC13* transcriptional levels by RT-qPCR. Fourteen and 19 samples expressed low and high levels of *ANAPC13*, respectively ($P < .0001$; Figure 5*A*). Next, copy number alterations (CNAs) were assessed using genomic DNA from the same sample set. A statistically significant association between low levels of *ANAPC13* and increased numbers of CNAs was observed ($P = .048$; Figure 5*B*). Breast tumor samples with low expression of this gene displayed 767 gains and 906 losses, whereas 355 gains and 377 losses were observed in the group of breast samples with high expression of *ANAPC13*. In these sample groups, no overrepresentation of any molecular subtypes was observed ($P = .36$; Table W9). Interestingly, the increased number of gains in samples expressing low levels of *ANAPC13* was mainly observed in the chromosomal regions where imbalances in breast tumor samples are frequently detected, such as gains at 1q (1q23.1-1q32.1), 8q, and 17q (17q24.2) [36] (Figure 5*C*).

We also used the aCGH data for checking whether the absence of *ANAPC13* protein in IDC samples could be a result of loss of *ANAPC13* chromosomal region. No *ANAPC13* losses were detected suggesting that other mechanisms are involved in the down-regulation of *ANAPC13* in breast tumor (Figure W1*B*).

Discussion

Ductal breast cancer progression is a multistep process in which continuous accumulation of molecular abnormalities leads to a series of histopathologic stages, namely flat epithelial atypia followed by atypical ductal hyperplasia, DCIS, and IDC, which may lead to metastatic disease and death [8,9]. In a cell-based microarray experiment, we observed that most of the molecular alterations in epithelial cells during breast cancer progression occur between cells of two morphologically similar lesions, pure DCIS and the *in situ* component of DCIS-IDC lesions, rather than between the *in situ* component of DCIS-IDC and IDC lesions, suggesting that molecular changes occur before the appearance of morphologic modifications [10]. By identifying changes in gene expression that precede DC invasion, we reasoned that is possible to unveil potential markers for clinical application, especially concerning the risk of progression of both pure DCIS and early-stage IDC lesions. Therefore, we examined changes in gene expression between pure DCIS and the *in situ* component of DCIS-IDC. We assessed eight genes, for which commercial antibodies are available, permitting the use of FFPE tissues for validation by IHC. That is especially important for pure DCIS lesions, which owing to their tiny size, are often entirely used for diagnosis proposals. This fact has hindered the identification of biomarkers for progression of pure DCIS, using frozen tissues for RNA-based analysis, considering the importance of assessing large and independent set of samples in the validation process. In addition, the low-quality RNA obtained from FFPE tissues can introduce bias in relative gene expression even with the improvements in the protocols for isolating RNA from FFPE tissue for assessing transcriptional data [37,38].

Among the eight genes tested, two, *ANAPC13* and *CLTCL1*, presented the potential to play an important role in DC progression. Both demonstrated decreased expression at both the mRNA and protein levels in the *in situ* component of DCIS-IDC lesions.

Differences in protein expression levels between the two types of preinvasive lesions, pure DCIS and the *in situ* component of DCIS-IDC, have also been reported by others [39,40]. ER, PR, and EGFR have been found to be more highly expressed in pure DCIS compared to *in situ* component of DCIS-IDC [40,41], reinforcing the existence of molecular differences between tumor cells from these two lesion types with similar morphology.

Table 3. ANAPC13 and CLTCL1 Expression (Cytoplasmic Staining) in a Tissue Microarray Composed IDC Samples.

Variable	Category	ANAPC13, *n* (%)*		*P*	CLTCL1, *n* (%)*		*P*
		Negative	Positive		Negative	Positive	
Lymph node metastasis	≤3	34 (32.00)	72 (68.00)	.09	30 (28.60)	75 (71.40)	.08
	>3	23 (46.00)	27 (54.00)		8 (16.00)	42 (84.00)	
In situ lesion	Absent	40 (50.00)	40 (50.00)	.24	19 (24.40)	59 (75.60)	.36
	Present	10 (37.00)	17 (63.00)		9 (33.30)	18 (67.70)	
ER status	Negative	24 (40.70)	35 (59.30)	.60	14 (23.30)	46 (76.70)	.83
	Positive	44 (36.70)	76 (63.30)		29 (24.80)	88 (75.20)	
PR status	Negative	42 (42.90)	56 (57.10)	.38	25 (25.00)	75 (75.00)	.83
	Positive	28 (36.40)	49 (63.60)		17 (23.60)	55 (76.40)	
HER2 status	Negative	54 (38.00)	88 (62.00)	.64	35 (25.00)	103 (75.00)	.89
	Positive	14 (42.00)	19 (58.00)		8 (24.00)	25 (76.00)	
EGFR	Negative	53 (38.00)	87 (62.00)	.90	32 (23.00)	106 (77.00)	.26
	Positive	11 (37.00)	19 (63.00)		9 (33.00)	18 (67.00)	
CK5/6	Negative	51 (39.00)	79 (61.00)	.99	27 (22.00)	98 (78.00)	.06
	Positive	17 (39.00)	27 (61.00)		16 (36.00)	29 (64.00)	
Nuclear grade	1	1 (50.00)	1 (50.00)	.96	1 (50.00)	1 (50.00)	.77
	2	19 (44.20)	24 (55.80)		11 (28.20)	28 (71.80)	
	3	48 (46.20)	56 (53.80)		28 (27.20)	75 (72.80)	
SBR grade	1	13 (44.80)	16 (55.20)	.98	9 (33.30)	18 (66.70)	.70
	2	40 (46.50)	46 (53.50)		24 (28.20)	61 (71.80)	
	3	15 (46.90)	17 (53.10)		7 (23.30)	23 (76.70)	
Clinical stage	I + II	34 (44.00)	44 (56.00)	.68	26 (30.00)	62 (70.00)	.08
	III + IV	34 (40.00)	50 (60.00)		15 (18.00)	67 (82.00)	

CK, cytokeratin; EGFR, epidermal growth factor receptor; ER, estrogen receptor; HER2, human epidermal growth factor receptor type 2; IDC, invasive ductal carcinoma; PR, progesterone receptor.
*Percentage considering number of cases with complete information.

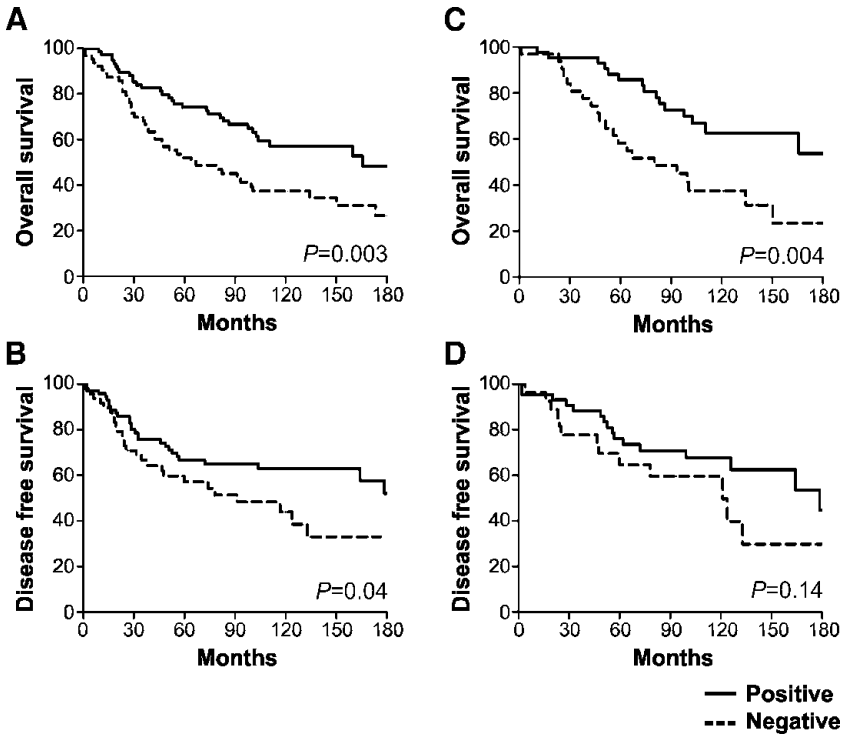

Figure 4. Kaplan-Meier survival curves based on ANAPC13 cytoplasmic staining. The overall survival time was defined as the interval between the beginning of treatment (surgery) and the date of death or the last information for censored observations. The disease-free interval was measured from the date of the treatment to the date when recurrence was diagnosed. The follow-up period varied from 1 to 180 months (73.8 ± 39.8, mean ± SD). A total of 64 recurrences were observed, and the time of these recurrences varied from 1 to 176.2 months (34.5 ± 38.6, mean ± SD). Overall survival (A) and disease-free survival (B) in patients positive or negative to ANAPC13 cytoplasmic staining with invasive ductal carcinoma. Overall survival (C) and disease-free survival (D) in luminal A group positive or negative to ANAPC13 cytoplasmic staining.

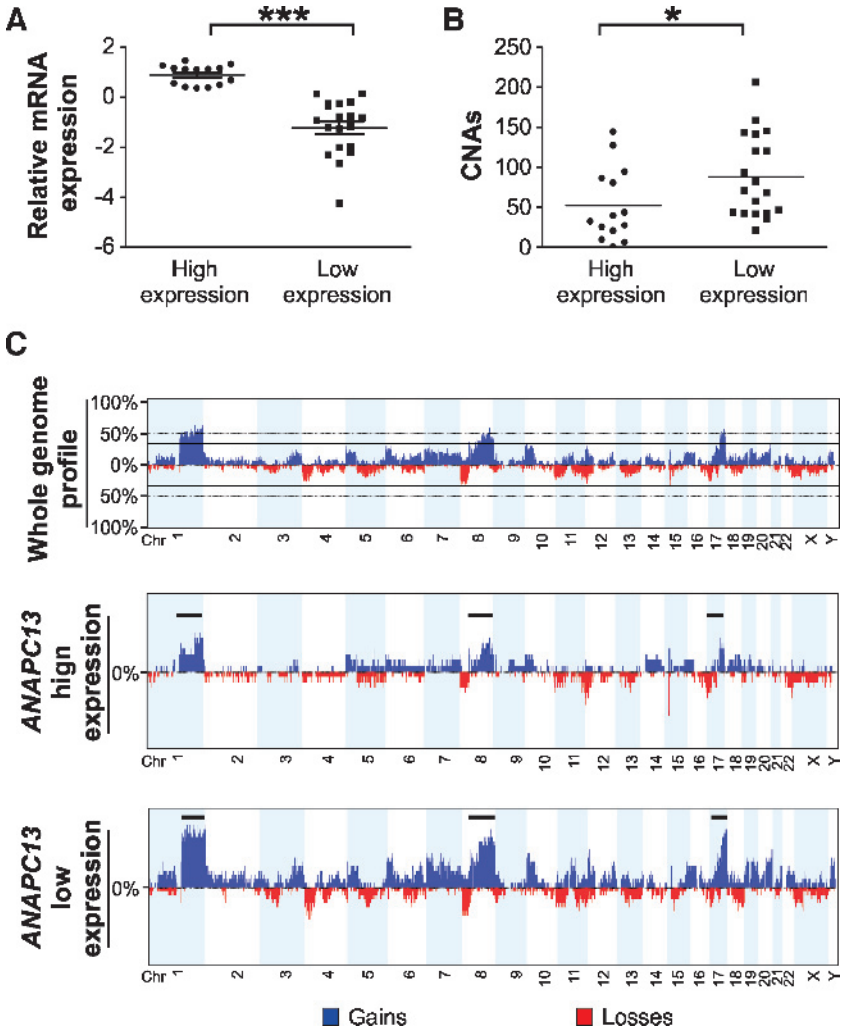

Figure 5. Correspondence between *ANAPC13* expression and genomic instability in invasive ductal carcinoma. (A) Relative mRNA expression in IDC cases with high and low expression of *ANAPC13* by RT-qPCR. (B) Number of CNAs in IDC samples with high and low expression of *ANAPC13*. (C) The *x* axis corresponds to the genomic region from chromosomes 1 to 22, X and Y, and the *y* axis represents the percentage of gains (plotted in blue above the 0% baseline) and losses (plotted in red below the 0% baseline) in all selected samples at the specified location in genome. The upper panel shows genome-wide CNAs (gains and losses) in 33 breast tumors. The middle and lower panels show frequency plots of breast tumors grouped according to *ANAPC13* expression status (high and low expression, respectively). Breast tumors with low *ANAPC13* expression show a distinctive pattern of genomic alterations mainly characterized by an increased frequency of gains at 1q (1q23.1-1q32.1), 8q, and 17q (17q24.2) (represented by black bars). Images obtained from Nexus copy number 5.1 software (Biodiscovery). Chr indicates chromosome; CNAs, copy number alterations. $^{*}P < .05$, $^{***}P < .001$.

The fact that *CLTCL1* expression decreases at the mRNA and protein levels in the earliest stages of tumor progression, when the cells still exhibit a preinvasive phenotype, but shows no further changes in expression during late stages of tumor progression highlights the potential of this gene as a biomarker for risk of progression of pure preinvasive lesions. Modulation of the expression of clathrins and/or clathrin adaptors seems to have a role in tumorigenesis and cell proliferation [42]. Although additional evidence of *CLTCL1* importance in the context of DCIS progression is necessary, the current analysis is the first study, to our knowledge, that associates *CLTCL1* with breast tumors.

The expression of *ANAPC13* decreased progressively at both the mRNA and protein levels during the course of tumor progression. Multivariate analyses associated positive ANAPC13 categories of breast tumors with higher rates of survival, suggesting that the presence of ANAPC13 may be a protective factor for patients with DC of the breast.

In overall survival, the protective effect of ANAPC13 expression was especially clear in luminal A cases, defined as ER- and/or PR-positive and HER2-negative. Although they are thought to have a good prognosis, luminal A breast tumors are a heterogeneous group including patients with distinct clinical outcomes. Therefore, the importance of novel molecular markers able to stratify tumors for more efficient and individualized treatment is obvious [43,44], and *ANAPC13* may have an important role in the subclassification of luminal A cases.

On the basis of the role of *ANAPC13*, as a subunit of APC/C complex, which is responsible for destroying the cohesion between sister chromatids by the activation of a protein called cysteine-protease separase, enabling the mitotic spindle to pull sister chromatids to opposite spindle poles [45], we decided to investigate the relation between *ANAPC13* expression and CNAs. A statistically significant association was observed between a low expression of *ANAPC13* and higher

number of CNAs. Triple-negative tumors are more likely to present genetic instability, and this is especially apparent in the basal-like subtype [36]. We did not observe overrepresentation of any of the molecular subtypes in either the *ANAPC13* high- or low-expressing groups, indicating that down-regulation of *ANAPC13* expression is probably associated to increased chromosomal instability in breast tumors.

ANAPC13 down-regulation does not seem to be a reflection of truncated proteins generated by non–sense mutation or frameshift mutation because no alterations in breast tumor DNA were observed in the coding sequence of this gene. Other mechanisms that regulate transcriptional expression, such as epigenetic modifications or microRNA, might be involved in the decrease of mRNA and protein expression levels.

Much attention has been focused on understanding how epithelial cells can survive in a hypoxic, nutrient-deprived *in situ* niche and how that niche in turn promotes genetic instability and triggers an invasive phenotype by selecting neoplastic cells with invasive capacity [14,46,47]. Although the current study demonstrates that tumors expressing low levels of *ANAPC13* harbored higher number of CNAs, the precise role played by *ANAPC13* in genomic instability remains to be addressed. A more thorough investigation of *ANAPC13* function in the context of breast cancer, especially its function in genomic instability, may contribute to the understanding of mechanisms underlying the progression of DC.

Together, the results presented in this study strongly suggest that the investigation of the molecular differences between epithelial tumor cells from pure DCIS and from the *in situ* component of DCIS-IDC, which are representative of the first molecular alterations that precede morphologic modifications, can result in the identification of novel molecular markers involved in the progression of ductal carcinoma of the breast.

Acknowledgments

The authors thank the Biobank, Centro Internacional de Pesquisa e Ensino the International Center of Research and Education at the A.C. Camargo Hospital. The authors thank Ricardo Renzo Brentani for critically reviewing this article.

References

[1] Berman HK, Gauthier ML, and Tlsty TD (2010). Premalignant breast neoplasia: a paradigm of interlesional and intralesional molecular heterogeneity and its biological and clinical ramifications. *Cancer Prev Res (Phila)* **3**, 579–587.

[2] Lagios MD (1995). Heterogeneity of duct carcinoma *in situ* (DCIS): relationship of grade and subtype analysis to local recurrence and risk of invasive transformation. *Cancer Lett* **90**, 97–102.

[3] Mokbel K and Cutuli B (2006). Heterogeneity of ductal carcinoma *in situ* and its effects on management. *Lancet Oncol* **7**, 756–765.

[4] Sgroi DC (2010). Preinvasive breast cancer. *Annu Rev Pathol* **5**, 193–221.

[5] Perou CM, Sorlie T, Eisen MB, van de Rijn M, Jeffrey SS, Rees CA, Pollack JR, Ross DT, Johnsen H, Akslen LA, et al. (2000). Molecular portraits of human breast tumours. *Nature* **406**, 747–752.

[6] Sorlie T, Perou CM, Tibshirani R, Aas T, Geisler S, Johnsen H, Hastie T, Eisen MB, van de Rijn M, Jeffrey SS, et al. (2001). Gene expression patterns of breast carcinomas distinguish tumor subclasses with clinical implications. *Proc Natl Acad Sci USA* **98**, 10869–10874.

[7] Bombonati A and Sgroi DC (2011). The molecular pathology of breast cancer progression. *J Pathol* **223**, 307–317.

[8] Wellings SR and Jensen HM (1973). On the origin and progression of ductal carcinoma in the human breast. *J Natl Cancer Inst* **50**, 1111–1118.

[9] Wellings SR, Jensen HM, and Marcum RG (1975). An atlas of subgross pathology of the human breast with special reference to possible precancerous lesions. *J Natl Cancer Inst* **55**, 231–273.

[10] Castro NP, Osorio CA, Torres C, Bastos EP, Mourao-Neto M, Soares FA, Brentani HP, and Carraro DM (2008). Evidence that molecular changes in cells occur before morphological alterations during the progression of breast ductal carcinoma. *Breast Cancer Res* **10**, 5/R87.

[11] Ma XJ, Salunga R, Tuggle JT, Gaudet J, Enright E, McQuary P, Payette T, Pistone M, Stecker K, Zhang BM, et al. (2003). Gene expression of human breast cancer progression. *Proc Natl Acad Sci USA* **100**, 5974–5979.

[12] Schuetz CS, Bonin M, Clare SE, Nieselt K, Sotlar K, Walter M, Fehm T, Solomayer E, Riess O, Wallwiener D, et al. (2006). Progression-specific genes identified by expression profiling of matched ductal carcinomas *in situ* and invasive breast tumors, combining laser capture microdissection and oligonucleotide microarray analysis. *Cancer Res* **66**, 5278–5286.

[13] Damonte P, Hodgson JG, Chen JQ, Young LJ, Cardiff RD, and Borowsky AD (2008). Mammary carcinoma behavior is programmed in the precancer stem cell. *Breast Cancer Res* **10**, 3/R50.

[14] Espina V and Liotta LA (2011). What is the malignant nature of human ductal carcinoma *in situ*? *Nat Rev Cancer* **11**, 68–75.

[15] Ma XJ, Dahiya S, Richardson E, Erlander M, and Sgroi DC (2009). Gene expression profiling of the tumor microenvironment during breast cancer progression. *Breast Cancer Res* **11**, 1/R7.

[16] Hu M and Polyak K (2008). Molecular characterisation of the tumour microenvironment in breast cancer. *Eur J Cancer* **44**, 2760–2765.

[17] Hu M, Yao J, Carroll DK, Weremowicz S, Chen H, Carrasco D, Richardson A, Violette S, Nikolskaya T, Nikolsky Y, et al. (2008). Regulation of *in situ* to invasive breast carcinoma transition. *Cancer Cell* **13**, 394–406.

[18] Schnitt SJ (2009). The transition from ductal carcinoma *in situ* to invasive breast cancer: the other side of the coin. *Breast Cancer Res* **11**, 1/101.

[19] Rozenchan PB, Carraro DM, Brentani H, de Carvalho Mota LD, Bastos EP, Ferreira EN, Torres CH, Katayama ML, Roela RA, Lyra EC, et al. (2009). Reciprocal changes in gene expression profiles of cocultured breast epithelial cells and primary fibroblasts. *Int J Cancer* **125**, 2767–2777.

[20] Yoon HJ, Feoktistova A, Wolfe BA, Jennings JL, Link AJ, and Gould KL (2002). Proteomics analysis identifies new components of the fission and budding yeast anaphase-promoting complexes. *Curr Biol* **12**, 2048–2054.

[21] Peters JM (2002). The anaphase-promoting complex: proteolysis in mitosis and beyond. *Molecular Cell* **9**, 931–943.

[22] Liu SH, Towler MC, Chen E, Chen CY, Song W, Apodaca G, and Brodsky FM (2001). A novel clathrin homolog that co-distributes with cytoskeletal components functions in the trans-Golgi network. *EMBO J* **20**, 272–284.

[23] Long KR, Trofatter JA, Ramesh V, McCormick MK, and Buckler AJ (1996). Cloning and characterization of a novel human clathrin heavy chain gene. *Genomics* **35**, 466–472.

[24] Hood FE and Royle SJ (2009). Functional equivalence of the clathrin heavy chains CHC17 and CHC22 in endocytosis and mitosis. *J Cell Sci* **122**, 2185–2190.

[25] Kedra D, Peyrard M, Fransson I, Collins JE, Dunham I, Roe BA, and Dumanski JP (1996). Characterization of a second human clathrin heavy chain polypeptide gene (*CLH-22*) from chromosome 22q11. *Hum Mol Genet* **5**, 625–631.

[26] Royle SJ, Bright NA, and Lagnado L (2005). Clathrin is required for the function of the mitotic spindle. *Nature* **434**, 1152–1157.

[27] Calmon MF, Rodrigues RV, Kaneto CM, Moura RP, Silva SD, Mota LD, Pinheiro DG, Torres C, de Carvalho AF, Cury PM, et al. (2009). Epigenetic silencing of CRABP2 and MX1 in head and neck tumors. *Neoplasia* **11**, 1329–1339.

[28] Hammond ME, Hayes DF, Dowsett M, Allred DC, Hagerty KL, Badve S, Fitzgibbons PL, Francis G, Goldstein NS, Hayes M, et al. (2010). American Society of Clinical Oncology/College of American Pathologists guideline recommendations for immunohistochemical testing of estrogen and progesterone receptors in breast cancer (unabridged version). *Arch Pathol Lab Med* **134**, 48–72.

[29] Wolff AC, Hammond ME, Schwartz JN, Hagerty KL, Allred DC, Cote RJ, Dowsett M, Fitzgibbons PL, Hanna WM, Langer A, et al. (2007). American Society of Clinical Oncology/College of American Pathologists guideline recommendations for human epidermal growth factor receptor 2 testing in breast cancer. *J Clin Oncol* **25**, 118–145.

[30] Khramtsov AI, Khramtsov MT, Tretiakova M, Huo D, Olapade OI, and Goss KH (2010). Wnt/catenin pathway activation is enriched in basal-like breast cancers and predicts poor outcome. *Am J Pathol* **176**, 2911–2920.

[31] Vandesompele J, De Preter K, Pattyn F, Poppe B, Van Roy N, De Paepe A, and Speleman F (2002). Accurate normalization of real-time quantitative RT-PCR data by geometric averaging of multiple internal control genes. *Genome Biol* **3**, RESEARCH0034.

[32] Pfaffl MW (2001). A new mathematical model for relative quantification in real-time RT-PCR. *Nucleic Acids Res* **29**, 2002–2007.

[33] Allred DC, Harvey JM, Berardo M, and Clark GM (1998). Prognostic and predictive factors in breast cancer by immunohistochemical analysis. *Mod Pathol* **11**, 155–168.

[34] Ricca TI, Liang G, Suenaga AP, Han SW, Jones PA, and Jasiulionis MG (2009). Tissue inhibitor of metalloproteinase 1 expression associated with gene demethylation confers anoikis resistance in early phases of melanocyte malignant transformation. *Transl Oncol* **2**, 329–340.

[35] Ferreira EN, Maschietto M, Silva SD, Brentani H, and Carraro DM (2010). Evaluation of quantitative RT-PCR using nonamplified and amplified RNA. *Diagn Mol Pathol* **19**, 45–53.

[36] Bergamaschi A, Kim YH, Wang P, Sorlie T, Hernandez-Boussard T, Lonning PE, Tibshirani R, Borresen-Dale AL, and Pollack JR (2006). Distinct patterns of DNA copy number alteration are associated with different clinicopathological features and gene-expression subtypes of breast cancer. *Genes Chromosomes Cancer* **45**, 1033–1040.

[37] Benchekroun M, DeGraw J, Gao J, Sun L, von Boguslawsky K, Leminen A, Andersson LC, and Heiskala M (2004). Impact of fixative on recovery of mRNA from paraffin-embedded tissue. *Diagn Mol Pathol* **13**, 116–125.

[38] Saraiva TF, Castro NP, Pineda PHB, Osório CABT, Camargo LP, Brentani HP, and Carraro DM (2006). Effects of oligo dT-T7 RNA primer in RNA amplification from paraffin-embedded tissue for microarray experiments. *Appl Cancer Res* **26**, 14–20.

[39] Meijnen P, Peterse JL, Antonini N, Rutgers EJ, and van de Vijver MJ (2008). Immunohistochemical categorisation of ductal carcinoma *in situ* of the breast. *Br J Cancer* **98**, 137–142.

[40] Steinman S, Wang J, Bourne P, Yang Q, and Tang P (2007). Expression of cytokeratin markers, ER-α, PR, HER-2/*neu*, and EGFR in pure ductal carcinoma *in situ* (DCIS) and DCIS with co-existing invasive ductal carcinoma (IDC) of the breast. *Ann Clin Lab Sci* **37**, 127–134.

[41] Schorr MC, Pedrini JL, Savaris RF, and Zettler CG (2010). Are the pure *in situ* breast ductal carcinomas and those associated with invasive carcinoma the same? *Appl Immunohistochem Mol Morphol* **18**, 51–54.

[42] Pyrzynska B, Pilecka I, and Miaczynska M (2009). Endocytic proteins in the regulation of nuclear signaling, transcription and tumorigenesis. *Mol Oncol* **3**, 321–338.

[43] Di CS and Baselga J (2010). Management of breast cancer with targeted agents: importance of heterogeneity. *Nat Rev Clin Oncol* **7**, 139–147.

[44] Loi S (2008). Molecular analysis of hormone receptor positive (luminal) breast cancers: what have we learnt? *Eur J Cancer* **44**, 2813–2818.

[45] Nasmyth K (2001). Disseminating the genome: joining, resolving, and separating sister chromatids during mitosis and meiosis. *Annu Rev Genet* **35**, 673–745.

[46] Bindra RS and Glazer PM (2005). Genetic instability and the tumor microenvironment: towards the concept of microenvironment-induced mutagenesis. *Mutat Res* **569**, 75–85.

[47] Mathew R, Karantza-Wadsworth V, and White E (2007). Role of autophagy in cancer. *Nat Rev Cancer* **7**, 961–967.

Table W1. Distribution of Breast Cancer Cases According to Clinicopathologic Variables.

Variable	Category	TMA 1 (Pure DCIS and DCIS-IDC), *n* (%)*	TMA 2 (Invasive Samples), *n* (%)*
Histologic type of DCIS	Pure DCIS	44 (55.00)	NA
	In situ component of DCIS-IDC	36 (45.00)	27 (14.40)
	IDC	NA	160 (85.60)
Histologic subtype	Non-comedo	62 (82.70)	ND
	Comedo	13 (17.30)	ND
Nuclear grade	1	4 (5.60)	2 (1.30)
	2	33 (46.50)	43 (28.30)
	3	34 (47.90)	107 (70.40)
Histologic grade	Non-high grade	34 (51.5)	ND
	High grade	32 (48.5)	ND
SBR grade	1	ND	29 (19.30)
	2	ND	89 (59.30)
	3	ND	32 (21.30)
Clinical stage	I + II	ND	78 (48.00)
	III + IV	ND	84 (52.00)
Estrogen receptor status	Negative	22 (32.80)	61 (33.20)
	Positive	45 (67.20)	123 (66.80)
Progesterone status	Negative	31 (46.27)	103 (57.20)
	Positive	36 (53.73)	77 (42.80)
HER2 status	Negative	11 (16.70)	145 (83.30)
	Positive	55 (83.30)	29 (16.70)
CK5/6	Negative	ND	130 (73.00)
	Positive	ND	48 (27.00)
EGFR	Negative	ND	144 (82.80)
	Positive	ND	30 (17.20)
Recurrence	No	ND	75 (52.82)
	Yes	ND	67 (47.18)
Lymph node metastasis	≤3	ND	108 (67.00)
	>3	ND	53 (33.00)
Adjuvant chemotherapy	No	ND	77 (54.2)
	Yes	ND	65 (45.8)
Radiotherapy	No	ND	37 (26.0)
	Yes	ND	105 (74.0)
Hormone therapy	No	ND	75 (52.8)
	Yes	ND	67 (47.2)

CK, cytokeratin; DCIS, ductal carcinoma *in situ*; DCIS-IDC, ductal carcinoma *in situ* with coexisting invasive ductal carcinoma; HER2, human epidermal growth factor receptor type 2; IDC, invasive ductal carcinoma; NA, not applicable; ND, not determined; SBR grade, Scarff-Bloom-Richardson grade; TMA, tissue microarray.
*Percentage considering the number of cases with complete information.

Table W2. Genes and Primer Sequences Used in RT-qPCR and Mutation Screening Analysis.

RT-qPCR Analysis			Mutation Analysis	
Gene Symbol	Annotation	Primer Sequences (5′-3′)	Primer Sequence	Exons Analyzed
ADFP (GenBank: NM_001122.2)	Adipose differentiation-related protein	Forward: GATACTGATGAGTCCCACTG Reverse: GGTACACCTTGGATGTTGG	Forward: CCAGCCTCTGTAGTCGG Reverse: GGGACACGTCTTATCAATTTC	1
ANAPC13 (GenBank: NM_015391.3)	Anaphase-promoting complex subunit 13	Forward: GATTGATGATGCTTGGCG Reverse: GTAAGGCTAAGTCTGTCC	Forward: GTACGGTGCGGATGGTG Reverse: CAGGGCACACTGATTATCTTG	1
ARHGAP19 (GenBank: NM_032900)	Rho GTPase activating protein 19	Forward: CAAGATTGAAGTGGTCTGAAG Reverse: CAAGATTGAAGTGGTCTGAAG	Forward: GGAGAGAGGAACTGTGATC Reverse: GTTAGAGAATTCCACAGCTTTG	2
CLTCL1 (GenBank: NM_01835.3)	Clathrin, heavy chain-like 1	Forward: GATGGGCATGAATGAGAC Reverse: CGAAGTTGGGAGCAGA	Forward: CCTAGGAACTCACAAGC Reverse: GCCTTTCCCTCTCATA	3
CPNE3 (GenBank: 003909.3)	Copine III	Forward: CGAAGTTGGGAGCAGAG Reverse: CTGCCAAGACACACTGAG	Forward: GCTGTCAAAGTTTAACACC Reverse: GGATGTATCTGGATTATAGG	3
IMMT (GenBank: 006839.2)	Inner membrane protein, mitochondrial	Forward: GATCACTTGCGAGATGTCC Reverse: GACTGAGACGACGAAATTG		
NGDN (GenBank: NM_001042635.1)	Neuroguidin, EIF4E binding protein	Forward: CGTTTTAAGCCTCATCCCAG Reverse: CATCTTCTGCTTCATCTTCCTC		
PIAS2 (GenBank: NM_0046712)	Protein inhibitor of activated STAT2	Forward: GACCGAAGAAAGAAGCTATG Reverse: GTCACTGAACAAGGCTTAC		
ACTB (GenBank: MN_001101.3)	Actin beta	Forward: GCACCCAGCACAATGAAG Reverse: CTTGCTGATCCACATCTGC		
BCR (GenBank: NM_004327)	Breakpoint cluster region	Forward: CCTTCGACGTCAATAACAAGGAT Reverse: CCTGCGATGGCGTTCAC		
GAPDH (GenBank: AJ00531)	Glyceraldehyde-3-phosphate dehydrogenase	Forward: GAAGGTGAAGGTCGGA Reverse: GGGTCATTGATGGCAAC		
HPRT1 (GenBank: NM_000194.2)	Hypoxanthine phosphoribosyltransferase 1	Forward: CCCACGAAGTGTTGGATATAAGC Reverse: GGGCATATCCTACAACAAACTTGTC		
RPLP0 (GenBank: NM_001002)	Hydrogenase expression/formation	Forward: GGAGACGGATTACACCTTC Reverse: CTTCAACCTTAGCTGGGG		

Table W3. ADFP, ANAPC13, ARHGAP19 and CLTCL1 Expression in a Tissue Microarray Composed of *In Situ* Lesions.

Protein	IHC Analysis	Histologic Type of DCIS		*P*
		Pure DCIS	*In Situ* Component of DCIS-IDC	
ADFP (cytoplasmic staining) (%)*	Negative	26 (68.40)	22 (73.30)	.28
	Positive	12 (31.60)	8 (26.70)	
ANAPC13 (nuclear staining) (%)*	Negative	13 (35.10)	10 (38.40)	.78
	Positive	24 (64.90)	16 (61.60)	
ANAPC13 (cytoplasmic staining) (%)*	Negative	11 (30.50)	16 (59.20)	.02†
	Positive	25 (69.50)	11 (40.80)	
ARHGAP19 (nuclear staining) (%)*	Negative	25 (71.40)	14 (50.00)	.08
	Positive	10 (28.60)	14 (50.00)	
ARHGAP19 (cytoplasmic staining) (%)*	Negative	11 (31.40)	8 (28.60)	.80
	Positive	24 (68.60)	20 (71.40)	
CLTCL1 (cytoplasmic staining) (%)*	Negative	14 (40.00)	20 (64.50)	.04†
	Positive	21 (60.00)	11 (35.50)	

DCIS indicates ductal carcinoma *in situ*; DCIS-IDC, ductal carcinoma *in situ* with coexisting invasive ductal carcinoma.
*Percentage considering the number of cases with complete information.
†$P < .05$.

Table W4. Association between Overall and Disease-Free Survival with ANAPC13 Cytoplasmic Expression.

Variable	Category	ANAPC13 (%)	
		Negative	Positive
Overall survival	5 years	50.4	73.0
	10 years	34.9	55.9
	15 years	21.4	33.8
Disease-free survival	5 years	51.8	63.2
	10 years	40.4	61.7
	15 years	31.4	50.8

Table W5. Independent Prognostic Factors According to the Cox Regression Model.

Variable	Category	Crude HR (95% IC)*	HR (95% IC)* Multivariate Analysis
SBR grade	1	1.0	1.0
	2	2.58 (1.2-5.3)	2.42 (1.1-5.2)
	3	3.60 (1.6-8.0)	4.29 (1.8-10.1)
T stage	T1 + T2	1.0	1.0
	T3 + T4	2.50 (1.5-4.1)	2.26 (1.3-3.9)
M stage	0	1.0	1.0
	1	5.77 (3.2-10.2)	4.11 (2.2-7.7)
ANAPC13 (cytoplasmic staining)	Positive	1.0	1.0
	Negative	2.00 (1.3-3.2)	2.09 (1.3-3.4)

HR indicates hazard ratio; M, metastasis; SBR grade, Scarff-Bloom-Richardson grade; T, tumor.
*Risks for death and 95% confidence interval.

Table W6. Association between ANAPC13 Cytoplasmic Staining and Clinicopathologic Variables in IDC Cases Classified According to the Molecular Classification (Luminal A and B).

Clinicopathologic Variable	Category	Luminal A		*P*	Luminal B		*P*
		Negative for ANAPC13 (%)*	Positive for ANAPC13 (%)*		Negative for ANAPC13 (%)*	Positive for ANAPC13 (%)*	
Lymph node metastasis	≤3	17 (28.30)	43 (71.70)	.01†	1 (25.00)	3 (75.00)	>.999
	>3	14 (56.00)	11 (44.00)		1 (33.30)	2 (66.70)	
Nuclear grade	1	1 (100.00)	0 (0.00)	NA	0 (0.00)	0 (0.00)	NA
	2	7 (35.00)	13 (65.00)		0 (0.00)	2 (100.00)	
	3	24 (41.40)	34 (58.60)		2 (50.00)	2 (50.00)	
In situ lesion	absent	18 (45.00)	22 (55.00)	.76	1 (50.00)	1 (50.00)	NA
	present	7 (50.00)	7 (50.00)		0 (0.00)	0 (0.00)	
SBR grade	1	7 (43.70)	9 (56.30)	.22	0 (0.00)	1 (100.00)	NA
	2	21 (47.70)	23 (52.30)		2 (50.00)	2 (50.00)	
	3	4 (23.50)	13 (76.50)		0 (0.00)	1 (100.00)	
Clinical stage	I + II	19 (40.00)	29 (60.00)	.85	2 (67.00)	1 (33.00)	.52
	III + IV	17 (38.00)	28 (62.00)		3 (33.00)	6 (67.00)	

IDC indicates invasive ductal carcinoma; NA, not applicable; SBR grade, Scarff-Bloom-Richardson grade.
*Percentage of cases with complete information.
†$P < .05$.

Table W7. Association between ANAPC13 Cytoplasmic Staining and Clinicopathologic Variables in IDC Cases Classified According to the Molecular Classification (HER2$^+$, Basal-like, and Unclassified).

Clinicopathologic Variable	Category	HER2$^+$		*P*	Basal-like		*P*	Unclassified		*P*
		Negative for ANAPC13 (%)*	Positive for ANAPC13 (%)*		Negative for ANAPC13 (%)*	Positive for ANAPC13 (%)*		Negative for ANAPC13 (%)*	Positive for ANAPC13 (%)*	
Lymph node metastasis	≤3	6 (50.00)	6 (50.00)	.31	3 (43.00)	4 (57.00)	NA	2 (20.00)	8 (80.00)	.06
	>3	1 (16.70)	5 (83.30)		0 (0.00)	2 (100.00)		5 (71.00)	2 (29.00)	
Nuclear grade	1	3 (50.00)	3 (50.00)	NA	0 (0.00)	0 (0.00)	NA	1 (50.00)	1 (50.00)	.20
	2	6 (46.20)	7 (53.80)		1 (50.00)	1 (50.00)		1 (33.00)	2 (67.00)	
	3	0 (0.00)	0 (0.00)		3 (33.00)	6 (67.00)		7 (47.00)	8 (53.00)	
In situ lesion	absent	6 (50.00)	6 (50.00)	>.999	2 (67.00)	1 (33.00)	>.999	4 (44.00)	5 (56.00)	>.999
	present	1 (50.00)	1 (50.00)		1 (50.00)	1 (50.00)		1 (50.00)	1 (50.00)	
SBR grade	1	3 (75.00)	1 (25.00)	.37	0 (0.00)	0 (0.00)	NA	1 (25.00)	3 (75.00)	.17
	2	3 (37.5)	5 (62.50)		2 (29.00)	5 (71.00)		7 (64.00)	4 (36.00)	
	3	2 (33.00)	4 (66.70)		2 (50.00)	2 (50.00)		1 (20.00)	4 (80.00)	
Clinical stage	I + II	4 (44.00)	5 (56.00)	>.999	1 (33.00)	2 (67.00)	>.999	7 (70.00)	3 (30.00)	.30
	III + IV	3 (43.00)	4 (57.00)		3 (43.00)	4 (57.00)		2 (33.00)	4 (67.00)	

IDC indicates invasive ductal carcinoma; NA, not applicable; SBR grade, Scarff-Bloom-Richardson grade.
*Percentage considering the number of cases with complete information.

Table W8. Genomic Alterations in *ANAPC13*.

Genomic Alteration	mRNA Region	Genotype	Frequency *n* = 42 (%)
c.–704G>C	5′UTR	Homozygous	27 (64.2%)
		Heterozygous	10 (23.8%)
c.–702_700 del GGG	5′UTR	Homozygous	36 (85.7%)
		Heterozygous	0 (0.0%)
c.–700 del G	5′UTR	Homozygous	1 (2.4%)
		Heterozygous	0 (0.0%)
c–531 C>G	5′UTR	Homozygous	1 (2.4%)
		Heterozygous	0 (0.0%)
c–662C>T	5′UTR	Homozygous	1 (2.4%)
		Heterozygous	0 (0%)
c.*3C>T	3′UTR	Homozygous	1 (2.4%)
		Heterozygous	0 (0%)
c.*193G>A	3′UTR	Homozygous	1 (2.4%)
		Heterozygous	0 (0.0%)

UTR indicates untranslated region.

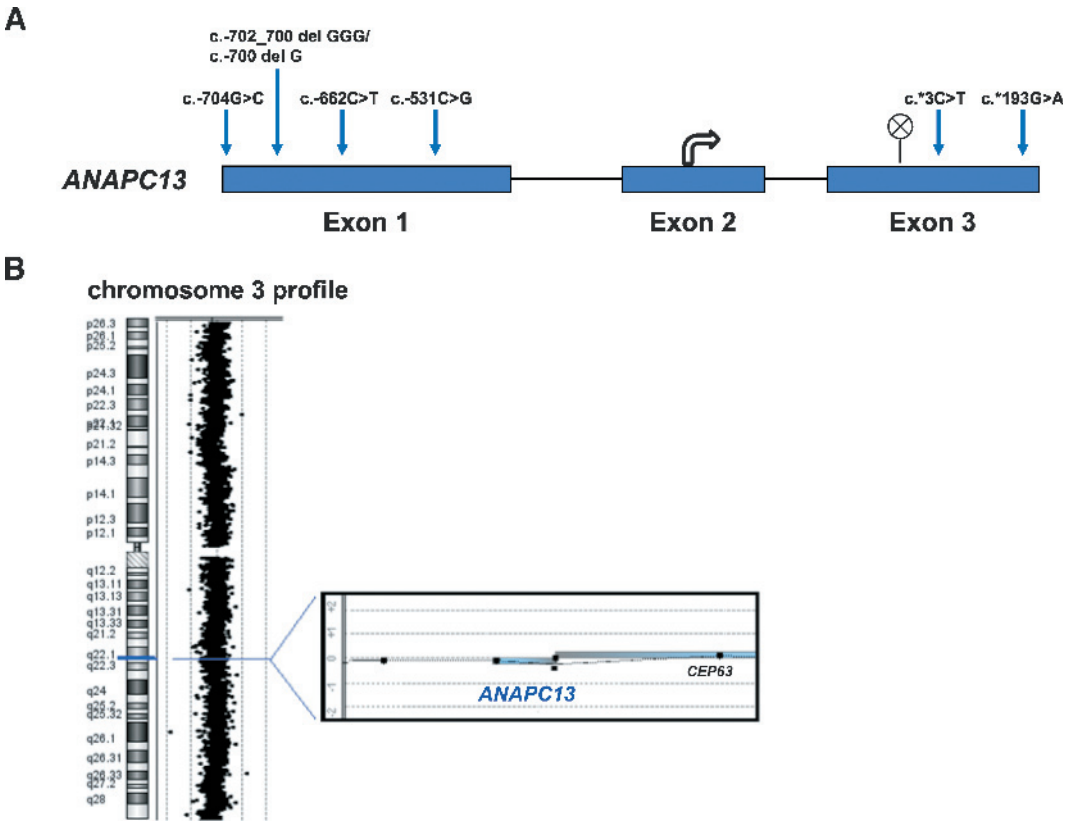

Figure W1. Mutation and deletion screening in *ANAPC13*. (A) Schematic representation of seven alterations found in *ANAPC13* genomic sequence. (B) Array CGH profile of a genomic segment at 3q22.2 from one sample of breast tumor. The figure depicts the location of the three oligoprobes mapped within the sequence of the gene *ANAPC13* (image extracted from the software Workbench DNA Analytics; Agilent Technologies). The values of log ratios around 0 showed that the investigated *ANAPC13* sequences had copy number equivalent to the whole genome of this tumor, suggesting that no deletions were observed.

Table W9. Analyses of *ANAPC13* Expression in Molecular Subtypes of Invasive Ductal Carcinoma.

Molecular Subtype	High Expression of *ANAPC13* (*n*%)	Low Expression of *ANAPC13* (*n*%)	*P*
Luminal A	6 (50.00)	6 (50.00)	.36
Luminal B	3 (75.00)	1 (25.00)	
HER2^{+}	2 (28.60)	5 (72.40)	
Triple-negative	3 (30.00)	7 (70.00)	